CENTRAL FINITE DIFFERENCE APPROACH TO FREE VIBRATIONS OF DOUBLE-TAPERED CANTILEVER BEAM WITH ELASTIC FOUNDATION AND TIP MASS

Nebojša Zdravković, Milomir Gašić, Mile Savković, Goran Marković
zdravkovic.n@mfkv.kg.ac.rs, gasic.m@mfkv.kg.ac.rs,
savkovic.m@mfkv.kg.ac.rs, markovic.g@mfkv.kg.ac.rs

University of Kragujevac, Faculty of Mechanical and Civil Engineering in Kraljevo
Dositejeva 19, 36000 Kraljevo
SERBIA

Key words: *free vibrations, double-tapered cantilever beam, finite difference method, Euler–Bernoulli theory, elastic foundation, tip mass.*

Abstract: *Free vibration problem of double-tapered cantilever beam with tip mass and elastically restrained root was solved efficiently and accurately by building a compact structure of algebraic equations, based on central finite difference method. Exact differential governing equation and boundary conditions were discretized by central finite differences applied upon grid points along the beam. Influence of support rigidity on mode shape function was discussed in term of discretized boundary equation. Boundary value problem was transformed in an appropriate matrix form, suitable for development of computational algorithms and solving with MATLAB routines. For a comparison purpose, a finite element method analysis was conducted in ANSYS. Testing cases were set up for numerous values of non-dimensional stiffness and mass parameters. Presented model yielded natural frequencies that were in a very good agreement with the results obtained from finite element simulation.*

1. INTRODUCTION

The extensive study of free bending vibration of non-uniform flexible beams started back few decades ago [1-5]. Since then, the issue of natural frequencies in bending vibrations of non-uniform flexible beams with various boundary conditions was studied in numerous cases and by different approaches and methods [6-21]. Yet, a fast-growing industry and infrastructure development force the mechanical and civil engineers to response promptly to new challenges in structural design with efficient but acceptably accurate solutions. At the same time, real-life tasks with their complexity usually impose the use of numerical approaches. Survey upon available literature revealed the fact that the finite difference method (FDM) was not employed as often as it deserved to be. AL-Sadder and AL-Rawi [22] used FDM for static large-deflection analysis of non-prismatic cantilever beams subjected to different types of continuous and discontinuous loadings, while Awrejcewicz et al. [23] studied regular and chaotic dynamics of the uniform Euler-Bernoulli beams and used FDM and finite element method (FEM) to verify the reliability of the obtained results.

This paper presents a detailed workflow of the FDM application to the eigenvalue problem of double-tapered beam in bending vibration. Presented approach yields a numerical scheme suitable for development of computational algorithms.

2. MODEL DESCRIPTION AND GOVERNING EQUATION

The model of double-tapered cantilever beam with tip mass and elastically restrained root considered herein is depicted in Fig.1. The motion under consideration is a free bending vibration of the beam in its symmetry plane *xy*. Transverse and axial displacements at supported end are fully restrained, while rotational restraint is elastic and presented by rotational spring with constant stiffness *k*. A lumped mass *M* is attached at the free end of the beam. The beam has a rectangular hollow cross-section with constant width *B* and wall thickness δ, while height *H(x)* and width *B(x)* linearly decrease towards its free end. Consequently, we have beam mass per unit length *m(x)* and the flexural rigidity *EI(x)* varying along length *L*, where *E* is Young's modulus of elasticity and *I(x)* is the cross-sectional moment of inertia about an axis normal to *x* and *y* and passing through the center of the cross section. The beam height and width in its root (*x=0*) are denoted as H_0 and B_0, while the free end height and width (*x=L*) are denoted as H_L and B_L.

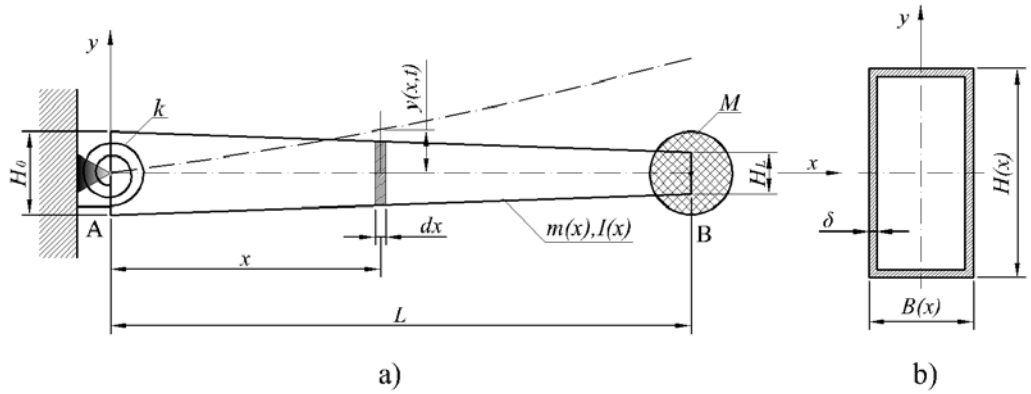

Fig.1. a Double-tapered cantilever beam with elastic support and tip mass b Cross-section

Analysis relies on Euler-Bernoulli beam theory, i.e. on the assumption that the rotatory inertia of the differential element and shear effects are negligible. The partial differential equation of motion for the free vibration of beams in bending, according to Euler-Bernoulli beam theory, is well known [24]

$$(1)\quad -\frac{\partial^2}{\partial x^2}\left[EI(x)\frac{\partial^2 y(x,t)}{\partial x^2}\right]=m(x)\frac{\partial^2 y(x,t)}{\partial t^2},\ 0\le x\le L$$

After differentiation, expanded form of Eq. (1) is

$$(2)\quad -E\left[\frac{d^2I(x)}{dx^2}\frac{\partial^2 y(x,t)}{\partial x^2}+2\frac{dI(x)}{dx}\frac{\partial^3 y(x,t)}{\partial x^3}+I(x)\frac{\partial^4 y(x,t)}{\partial x^4}\right]=m(x)\frac{\partial^2 y(x,t)}{\partial t^2}$$

Free vibration is harmonic, so the transverse displacement of the beam can be expressed in the form

$$(3)\quad y(x,t)=CY(x)\cos(\omega t-\varphi),\ 0\le x\le L$$

where *C* is amplitude, *Y(x)* is a mode shape function, ω is circular natural frequency and φ is a phase angle. Inserting Eq. (3) into Eq. (2) and dividing through by *Ccos(ωt-φ)*, we obtain the differential eigenvalue problem for Euler-Bernoulli non-uniform beam in bending

$$(4)\quad E\left[\frac{d^2I(x)}{dx^2}\frac{d^2Y(x)}{dx^2}+2\frac{dI(x)}{dx}\frac{d^3Y(x)}{dx^3}+I(x)\frac{d^4Y(x)}{dx^4}\right]=m(x)\omega^2Y(x)$$

In this case, the height and width of the double-tapered beam cross-section at the position of the differential element are as follows

$$(5)\quad H(x)=H_0-\eta x\,;\ B(x)=B_0-\mu x$$

where $\eta=(H_0-H_L)/L$ is non-dimensional height decrement and $\mu=(B_0-B_L)/L$ is non-dimensional width decrement. Therefore, the cross-sectional area becomes

$$(6)\quad A(x)=B(x)H(x)-\left[B(x)-2\delta\right]\left[H(x)-2\delta\right]=2\delta(H_0-\eta x+B_0-\mu x-2\delta)$$

and the mass per unit length, where ρ is material density, has the form

(7) $m(x) = 2\rho\delta(H_0 - \eta x + B_0 - \mu x - 2\delta)$

The cross-sectional moment of inertia is

(8) $I(x) = \frac{1}{12}\left\{B(x)H(x)^3 - [B(x) - 2\delta][(H(x) - 2\delta]^3\right\}$

After finding the needed derivatives out of Eq. (8) and inserting them and Eq. (7) into Eq. (4), we obtain a fully expanded differential governing equation for the beam under consideration

(9) $$\frac{1}{12}\left[BH^3 - (B-2\delta)(H-2\delta)^3\right]\frac{d^4Y}{dx^4} + \frac{1}{6}\left[-\mu H^3 - 3\eta BH^2 + \mu(H-2\delta)^3 + 3\eta(B-2\delta)(H-2\delta)^2\right]\frac{d^3Y}{dx^3} +$$
$$+\eta\delta(2\mu H + \eta B + \eta H)\frac{d^2Y}{dx^2} = \frac{2\rho\delta\omega^2}{E}(H + B - 2\delta)Y$$

3. BOUNDARY CONDITIONS

The solution *Y(x)* of Eq. (9) must satisfy two boundary conditions at each end. To obtain equations of boundary conditions in term of displacement *y(x,t)*, we recall the displacement relations to bending moment *M(x,t)* and shearing force *Q(x,t)* from mechanics of materials

(10) $M(x,t) = EI(x)\frac{\partial^2 y(x,t)}{\partial x^2}; Q(x,t) = -\frac{\partial}{\partial x}\left[EI(x)\frac{\partial^2 y(x,t)}{\partial x^2}\right]$

At the supported end, the displacement function *y(x,t)* has a zero value, while its slope outcomes from a ratio between bending moment and stiffness of the rotational spring

(11) $y(0,t) = 0$

(12) $\frac{\partial y(x,t)}{\partial x} = \frac{M(x,t)}{k} = \frac{E}{k}I(x)\frac{\partial^2 y(x,t)}{\partial x^2}, x = 0$

Assuming that moment of inertia of attached mass *M* about an axis normal to *x* and *y* is negligible, two boundary conditions for free end are as follows

(13) $M(x,t) = EI(x)\frac{\partial^2 y(x,t)}{\partial x^2} = 0, x = L$

(14) $Q(x,t) = -\frac{\partial}{\partial x}\left[EI(x)\frac{\partial^2 y(x,t)}{\partial x^2}\right] = -M\frac{\partial^2 y(x,t)}{\partial t^2}, x = L$

All boundary conditions written in term of mode shape function *Y(x)* and its derivatives are

(15) $Y(0) = 0$

(16) $Y'(0) = \frac{EI_0}{k}Y''(0)$

(17) $Y''(L) = 0$

(18) $\frac{dI(L)}{dx}Y''(L) + I(L)Y'''(L) + \frac{M\omega^2}{E}Y(L) = 0$

where $I_0 = I(x=0)$ and $I_L = I(x=l)$ are cross-sectional moments of inertia at the root and free end of the beam, respectively.

4. DISCRETIZATION OF BOUNDARY VALUE PROBLEM BY CENTRAL FINITE DIFFERENCES

Fig. 2 shows central finite difference grid scheme where the length of the beam *L* is equally divided by *n*+1 grid points into *n* segments with length $\Delta s = L/n$. To apply the method, there are three fictitious grid points added to the scheme, one before the root grid point and two after free-end grid point.

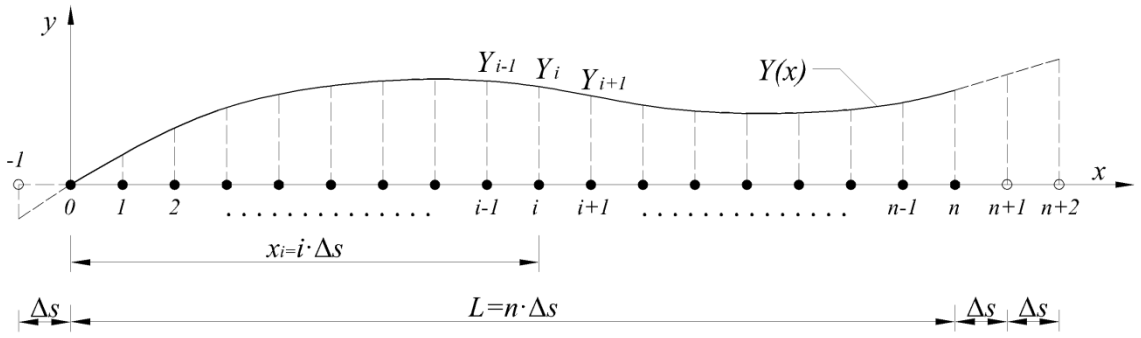

Fig.2. Central finite difference grid used for discretization of boundary value problem

Central finite difference approximations for derivatives of shape function *Y(x)* for grid point *i* are as follows

(19) $$\left(\frac{dY}{dx}\right)_i = Y_i' \approx \frac{-Y_{i-1}+Y_{i+1}}{2\Delta s}$$

(20) $$\left(\frac{d^2Y}{dx^2}\right)_i = Y_i'' \approx \frac{Y_{i-1}-2Y_i+Y_{i+1}}{(\Delta s)^2}$$

(21) $$\left(\frac{d^3Y}{dx^3}\right)_i = Y_i''' \approx \frac{-Y_{i-2}+2Y_{i-1}-2Y_{i+1}+Y_{i+2}}{2(\Delta s)^3}$$

(22) $$\left(\frac{d^4Y}{dx^4}\right)_i = Y_i^{IV} \approx \frac{Y_{i-2}-4Y_{i-1}+6Y_i-4Y_{i+1}+Y_{i+2}}{(\Delta s)^4}$$

4.1 Governing equation

Inserting Eqs. (19-22) into the governing equation Eq. (9) and putting $x=i\cdot\Delta s$, we obtain

(23) $$\begin{aligned}&E\left[BH^3-(B-2\delta)(H-2\delta)^3\right](Y_{i-2}-4Y_{i-1}+6Y_i-4Y_{i+1}+Y_{i+2})+\\&+E\Delta s\left[-\mu H^3-3\eta BH^2+\mu(H-2\delta)^3+3\eta(B-2\delta)(H-2\delta)^2\right](-Y_{i-2}+2Y_{i-1}-2Y_{i+1}+Y_{i+2})+\\&+12\eta\delta(\Delta s)^2E(2\mu H+\eta B+\eta H)(Y_{i-1}-2Y_i+Y_{i+1})-24\rho\delta\omega^2(\Delta s)^4(H+B-2\delta)Y_i=0;\ i=1,...,n\end{aligned}$$

Eq. (23) represents a system of *n* linear algebraic equations, with discreet values of shape function at the grid points positions Y_i as unknowns. Furthermore, by introducing the expressions

(24) $$\begin{aligned}P_i &= E\left[BH^3-(B-2\delta)(H-2\delta)^3\right]\\Q_i &= E\Delta s\left[-\mu H^3-3\eta BH^2+\mu(H-2\delta)^3+3\eta(B-2\delta)(H-2\delta)^2\right]\\R_i &= 12\eta\delta(\Delta s)^2E(2\mu H+\eta B+\eta H)\\S_i &= 24\rho\delta(H+B-2\delta)\end{aligned}$$

and parameter $\lambda=\omega^2(\Delta s)^4$, we rewrite Eq. (23) in more condensed form

(25) $$\begin{aligned}&(P_i-Q_i)Y_{i-2}-(4P_i-2Q_i-R_i)Y_{i-1}+(6P_i-2R_i-\lambda S_i)Y_i-\\&-(4P_i+2Q_i-R_i)Y_{i+1}+(P_i+Q_i)Y_{i+2}=0;\ i=1,...,n\end{aligned}$$

4.2 Boundary conditions

By inserting Eqs. (19-22) into Eqs. (15-18), we establish the expressions for fictitious grid points displacements in terms of displacements of real grid points at the boundaries. Hence, this will enable their elimination from the system later on. Those expressions are

(26) $$Y_0=0$$

(27) $$Y_{-1} = -\frac{2EI_0 - k\Delta s}{2EI_0 + k\Delta s} Y_1$$

(28) $$Y_{n+1} = 2Y_n - Y_{n-1}$$

(29) $$Y_{n+2} = Y_{n-2} - 4Y_{n-1} + \left[4 - \frac{2\lambda M}{\Delta s EI_L} \right] Y_n$$

4.3 Characteristic equation

Converting the constituent differential equations through discretization, we combine them and form the algebraic eigenvalue problem. In fact, by insertion of boundary conditions (26-29) into Eqs. (25) we eliminate fictitious displacements Y_{-1}, Y_{n+1} and Y_{n+2}, which yields a set of n algebraic equations with Y_i, $i=1,\ldots,n$ as unknowns and λ as a parameter. Boundary conditions affect the form of equations for first two and last two grid points only, while equations for all other internal grid points retain general form presented by Eqs. (25). We introduce following expressions

(30) $$T = \frac{2EI_0 - k\Delta s}{2EI_0 + k\Delta s} \text{ and } J = \frac{2M}{\Delta s EI_L}(P_n + Q_n)$$

and write the system of equations in the following form

$$i = 1: \frac{1}{S_1}\left\{\left[6P_1 - 2R_1 - T(P_1 - Q_1)\right]Y_1 - (4P_1 + 2Q_1 - R_1)Y_2 + (P_1 + Q_1)Y_3\right\} = \lambda Y_1$$

$$i = 2: \frac{1}{S_2}\left\{-(4P_2 - 2Q_2 - R_2)Y_1 + 2(3P_2 - R_2)Y_2 - (4P_2 + 2Q_2 - R_2)Y_3 + (P_2 + Q_2)Y_4\right\} = \lambda Y_2$$

(31) $$i = 3 \div n-2: \frac{1}{S_i}\left\{(P_i - Q_i)Y_{i-2} - (4P_i - 2Q_i - R_i)Y_{i-1} + 2(3P_i - R_i)Y_i - (4P_i + 2Q_i - R_i)Y_{i+1} + (P_i + Q_i)Y_{i+2}\right\} = \lambda Y_i$$

$$i = n-1: \frac{1}{S_{n-1}}\left\{(P_{n-1} - Q_{n-1})Y_{n-3} - (4P_{n-1} - 2Q_{n-1} - R_{n-1})Y_{n-2} + (5P_{n-1} - 2R_{n-1} - Q_{n-1})Y_{n-1} - (2P_{n-1} - R_{n-1})Y_n\right\} = \lambda Y_{n-1}$$

$$i = n: \frac{1}{S_n + J}(2P_nY_{n-2} - 4P_nY_{n-1} + 2P_nY_n) = \lambda Y_n$$

Previous form is convenient to formulate the eigenvalue problem as a matrix equation

(32) $$\mathbf{AY} = \lambda \mathbf{Y}$$

i.e.

(33) $$\left(\mathbf{A} - \lambda \mathbf{I_n}\right)\mathbf{Y} = 0$$

where $\boldsymbol{A}$ is a diagonal matrix, I_n is a unit matrix of size n, λ is an eigenvalue and $\boldsymbol{Y}$ is a column matrix of displacements that form mode shape. Nontrivial solutions exist if and only if the determinant of the coefficients is equal to zero, which finally leads to characteristic equation

(34) $$\Delta(\lambda) = \det\left[\mathbf{A} - \lambda \mathbf{I_n}\right] = 0$$

Finding the roots λ_i, $i=1,\ldots,n$ of Eq. (34) we find natural frequencies of the beam

(35) $$f_i = \frac{\omega_i}{2\pi} = \frac{\sqrt{\lambda_i}}{2\pi(\Delta s)^2} = \frac{n^2\sqrt{\lambda_i}}{2\pi L^2}, i = 1,\ldots n.$$

5. NUMERICAL EXAMPLE AND COMPARISON WITH FINITE ELEMENT MODEL

To investigate the accuracy of results obtained by FDM, a calculation is carried out through numerical example with following parameters: $L=3m$, $H_L=0.1m$, $B_L=0.1m$, $H_0=0.2m$, $B_0=0.2m$, $\delta=0.005m$, $\rho=7850kg/m^3$, $E=2.1\cdot10^{11}N/m^2$. The length of the beam is divided by $n=100$ grid points.

As it is more convenient to analyze the results in terms of relations of the quantities rather than in terms of themselves, we introduce the following stiffness and mass non-dimensional ratios

(36) $q = \dfrac{kL}{EI_0}$ and $r = \dfrac{M}{m}$

and where m is the self-mass of the beam. Hence, the expressions (30) derived from boundary conditions now become

(37) $T = \dfrac{2n-q}{2n+q}$ and $J = \dfrac{2rm}{\Delta s EI_L}(P_n + Q_n)$.

Numerical calculations within FDM approach were carried out by MATLAB software routines. On the other hand, we used a FEM analysis and ANSYS software to verify the results.

The numerical investigation was conducted in a manner where the value of stiffness ratio was gradually increased while mass ratio took values *r=0.5;1.0;1.5;2.0* repeatedly for each instance of stiffness ratio. Fig. 3 shows first three mode shapes and natural frequencies of the tapered beam in FEM analysis for the case where non-dimensional ratios take values *q=7.0* and *r=1.0* (highlighted fields in Table1).

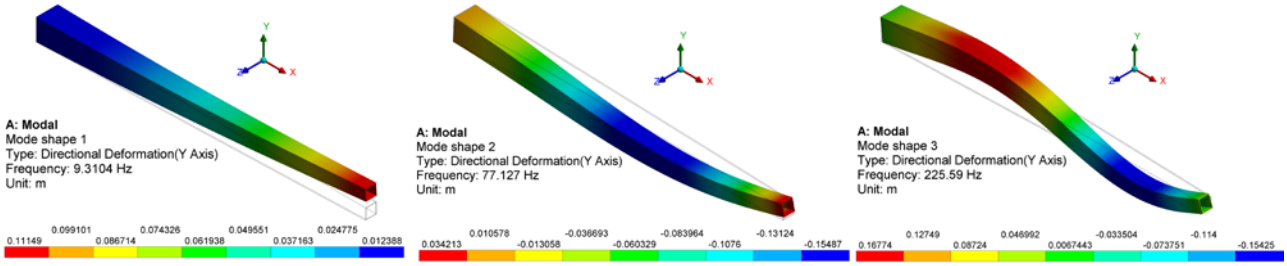

Fig. 3 First three mode shapes and natural frequencies from ANSYS for *q=7.0* and *r=1.0*

Table 1 shows the results for the first three natural frequencies obtained by both FDM and FEM analysis and corresponding relative deviations (columns Δ_1, Δ_2, Δ_3). A comparison between the results obtained by presented FDM approach and FEM analysis reveals very good agreement. Relative deviation for fundamental natural frequency does not exceed 1%, while for the second and third frequency it is about 2% and 7%, respectively. Since the effects of rotary inertia and shear deformation are neglected in the Euler–Bernoulli beam theory, the Euler–Bernoulli model always overestimates the natural frequency of free vibration [25]. Fig. 4 shows the dependencies of first three natural frequencies on various boundary conditions in terms of non-dimensional stiffness and mass ratios q and r. Increasing the value of stiffness ratio q makes the boundary condition at the root of the beam progressively approaches the clamped support type, which results in higher natural frequencies. Simultaneously, as expected, higher values of ratio between tip-mass and self-mass of the beam r make natural frequencies decrease.

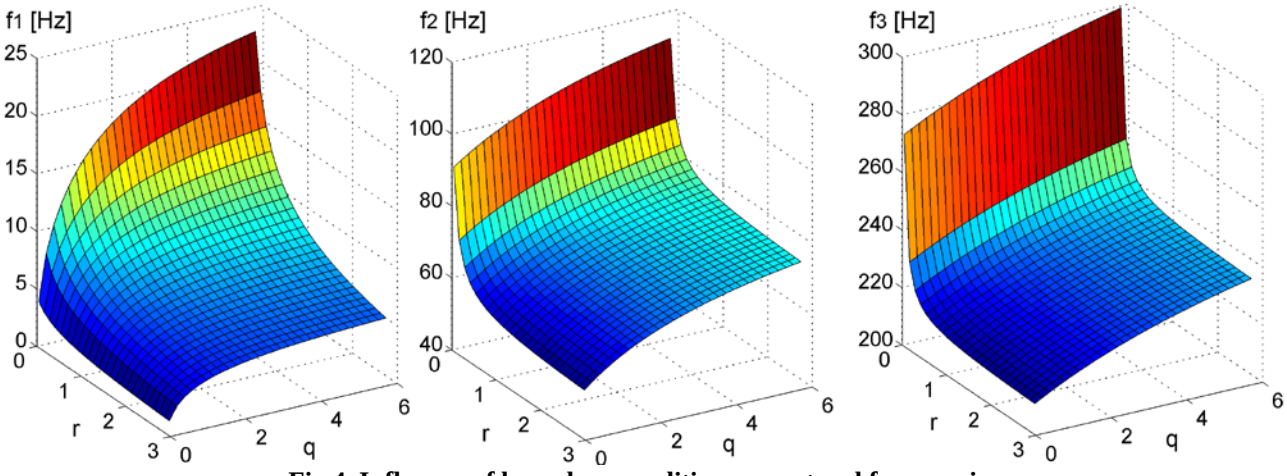

Fig.4. Influence of boundary conditions on natural frequencies

Table 1 First three natural frequencies obtained by FDM and FEM with relative deviations

		f_1			f_2			f_3		
q	r	FDM [Hz]	FEM [Hz]	Δ_1	FDM [Hz]	FEM [Hz]	Δ_2	FDM [Hz]	FEM [Hz]	Δ_1
0.25	0.50	4.58	4.54	0.80%	60.90	60.32	0.97%	216.86	206.09	5.22%
	1.00	3.56	3.53	0.86%	57.51	57.01	0.89%	213.70	203.17	5.18%
	1.50	3.01	2.98	0.88%	56.22	55.74	0.86%	212.58	202.13	5.17%
	2.00	2.66	2.63	0.90%	55.53	55.07	0.84%	212.01	201.60	5.16%
0.50	0.50	6.16	6.11	0.80%	62.70	62.04	1.06%	218.56	207.53	5.31%
	1.00	4.77	4.73	0.86%	59.40	58.82	0.98%	215.42	204.62	5.28%
	1.50	4.03	4.00	0.88%	58.14	57.59	0.95%	214.30	203.59	5.26%
	2.00	3.56	3.53	0.89%	57.47	56.94	0.94%	213.73	203.06	5.26%
1.00	0.50	8.00	7.93	0.81%	65.79	65.00	1.22%	221.71	210.18	5.49%
	1.00	6.16	6.11	0.85%	62.61	61.90	1.15%	218.59	207.30	5.45%
	1.50	5.20	5.15	0.86%	61.41	60.73	1.12%	217.49	206.27	5.44%
	2.00	4.58	4.54	0.87%	60.78	60.11	1.11%	216.92	205.75	5.43%
1.50	0.50	9.10	9.02	0.81%	68.37	67.45	1.36%	224.57	212.56	5.65%
	1.00	6.99	6.93	0.84%	65.26	64.43	1.29%	221.48	209.70	5.62%
	1.50	5.88	5.83	0.86%	64.09	63.29	1.27%	220.38	208.69	5.60%
	2.00	5.18	5.13	0.87%	63.48	62.70	1.25%	219.82	208.17	5.60%
2.00	0.50	9.85	9.77	0.81%	70.53	69.51	1.48%	227.18	214.71	5.81%
	1.00	7.54	7.48	0.84%	67.48	66.54	1.41%	224.10	211.88	5.77%
	1.50	6.35	6.29	0.85%	66.34	65.43	1.39%	223.01	210.87	5.75%
	2.00	5.58	5.53	0.85%	65.74	64.84	1.38%	222.45	210.35	5.75%
3.00	0.50	10.82	10.73	0.80%	73.98	72.77	1.67%	231.73	218.44	6.08%
	1.00	8.26	8.19	0.83%	70.99	69.87	1.61%	228.67	215.63	6.05%
	1.50	6.94	6.88	0.84%	69.87	68.78	1.58%	227.59	214.64	6.03%
	2.00	6.10	6.04	0.84%	69.28	68.21	1.57%	227.03	214.13	6.03%
4.00	0.50	11.42	11.33	0.80%	76.60	75.24	1.82%	235.56	221.55	6.32%
	1.00	8.70	8.63	0.83%	73.63	72.36	1.76%	232.52	218.76	6.29%
	1.50	7.30	7.24	0.83%	72.53	71.29	1.74%	231.44	217.77	6.28%
	2.00	6.41	6.36	0.84%	71.95	70.73	1.72%	230.89	217.27	6.27%
5.00	0.50	11.84	11.74	0.80%	78.66	77.16	1.94%	238.82	224.17	6.54%
	1.00	9.00	8.93	0.82%	75.70	74.30	1.88%	235.79	221.40	6.50%
	1.50	7.55	7.49	0.82%	74.60	73.24	1.85%	234.72	220.42	6.49%
	2.00	6.63	6.57	0.83%	74.02	72.69	1.84%	234.17	219.91	6.48%
7.00	0.50	12.37	12.27	0.80%	81.66	79.97	2.11%	244.06	228.34	6.88%
	1.00	9.39	**9.31**	0.81%	78.71	**77.13**	2.05%	241.04	**225.59**	6.85%
	1.50	7.86	7.80	0.82%	77.62	76.07	2.03%	239.97	224.61	6.84%
	2.00	6.90	6.85	0.82%	77.04	75.52	2.02%	239.42	224.11	6.83%
9.00	0.50	12.69	12.59	0.79%	83.76	81.93	2.23%	248.06	231.51	7.15%
	1.00	9.62	9.54	0.81%	80.80	79.08	2.17%	245.04	228.76	7.12%
	1.50	8.06	7.99	0.81%	79.71	78.03	2.15%	243.98	227.79	7.11%
	2.00	7.07	7.01	0.82%	79.13	77.48	2.14%	243.43	227.29	7.10%
10.00	0.50	12.81	12.71	0.80%	84.58	82.69	2.28%	249.73	232.81	7.27%
	1.00	9.71	9.63	0.81%	81.62	79.85	2.22%	246.71	230.07	7.23%
	1.50	8.13	8.06	0.81%	80.53	78.79	2.20%	245.64	229.10	7.22%
	2.00	7.13	7.07	0.81%	79.96	78.24	2.19%	245.10	228.61	7.21%

6. CONCLUSION

Differential eigenvalue problem of double-tapered cantilever beam with elastically restrained root and tip mass was efficiently solved by building a stable and compact structure of algebraic equations derived from FDM approach. The results for first three natural frequencies revealed very good agreement with the results obtained by FEM simulation in ANSYS.

After setting up a system of equations out of differential governing equation and boundary conditions through the process of discretization, presented numeric model pays back through its advantages. Firstly, equations written for all internal grid points that are not affected by discretized boundary conditions makes the model compact and convenient for development of software routines, e.g. in MATLAB. This feature opens additional possibilities for the research of the model

behavior in variety of cases with different values of non-dimensional stiffness, mass and taper ratios. Therefore, presented approach with FDM provides us an excellent control of system parameters in particular engineering applications.

Acknowledgments

This work was supported by the Ministry of Education, Science and Technological Development of the Republic of Serbia (Project TR35038).

References

[1] Laura PAA, Gutierrez RH. Vibrations of an elastically restrained cantilever beam of varying cross-section with tip mass of finite length. Journal of Sound and Vibration 108(1), 123–131 (1986).
[2] W.L. Craver Jr., P. Jampala. Transverse Vibrations of a Linearly Tapered Cantilever Beam With Constraining Springs. Journal of Sound and Vibration 166(3), 521–529 (1993).
[3] R.O. Grossi, B. del V. Arenas. A variational approach to the vibration of tapered beams with elastically restrained ends. Journal of Sound and Vibration 195(3), 507–511 (1996).
[4] N.M. Auciello. Transverse vibrations of a linearly tapered cantilever beam with tip mass of rotatory inertia and eccentricity. Journal of Sound and Vibration 194(1), 25–34 (1996).
[5] N.M. Auciello, G. Nolè. Vibrations of a cantilever tapered beam with varying section properties and carrying a mass at the free end. Journal of Sound and Vibration 214(1), 105–119 (1998).
[6] D. Zhou, Y.K. Cheung. The free vibration of a type of tapered beams. Computer Methods in Applied Mechanics and Engineering. 188, 203–216 (2000).
[7] N.M. Auciello. On the transverse vibrations of non-uniform beams with axial loads and elastically restrained ends. International Journal of Mechanical Sciences 43, 193–208 (2001)
[8] S. Naguleswaran. Vibration of an Euler–Bernoulli beam on elastic end supports and with up to three step changes in cross-section. International Journal of Mechanical Sciences 44, 2541–2555 (2002)
[9] S. Naguleswaran. Vibration and stability of an Euler–Bernoulli beam with up to three-step changes in cross-section and in axial force. International Journal of Mechanical Sciences 45, 1563–1579 (2003)
[10] Q.S. Li, L.F. Yang, Y.L. Zhao, G.Q. Li. Dynamic analysis of non-uniform beams and plates by finite elements with generalized degrees of freedom. International Journal of Mechanical Sciences 45, 813–830 (2003)
[11] H. Qiao, Q.S. Li, G.Q. Li. Vibratory characteristics of flexural non-uniform Euler–Bernoulli beams carrying an arbitrary number of spring–mass systems. International Journal of Mechanical Sciences 44, 725–743 (2002)
[12] Jong-Shyong Wu, Chin-Tzu Chen. An exact solution for the natural frequencies and mode shapes of an immersed elastically restrained wedge beam carrying an eccentric tip mass with mass moment of inertia. Journal of Sound and Vibration 286, 549–568 (2005)
[13] Michael A. Koplow, Abhijit Bhattacharyya, Brian P. Mann. Closed form solutions for the dynamic response of Euler–Bernoulli beams with step changes in cross section. Journal of Sound and Vibration 295, 214–225 (2006)
[14] R.D. Firouz-Abadi, H. Haddadpour, A.B. Novinzadeh. An asymptotic solution to transverse free vibrations of variable-section beams. Journal of Sound and Vibration 304, 530–540 (2007)
[15] J.W. Jaworski, E.H. Dowell. Free vibration of a cantilevered beam with multiple steps: Comparison of several theoretical methods with experiment. Journal of Sound and Vibration 312, 713–725 (2008)
[16] M.S. Abdel-Jaber et al. Nonlinear natural frequencies of an elastically restrained tapered beam. Journal of Sound and Vibration 313, 772–783 (2008)

[17] Jung-Chang Hsu, Hsin-Yi Lai, C.K. Chen. Free vibration of non-uniform Euler–Bernoulli beams with general elastically end constraints using Adomian modified decomposition method. Journal of Sound and Vibration 318, 965–981 (2008)
[18] E. J. Sapountzakis, D. G. Panagos. Nonlinear analysis of beams of variable cross section, including shear deformation effect. Archive of Applied Mechanics. 78, 687–710 (2008)
[19] Yong Huang, Xian-Fang Li. A new approach for free vibration of axially functionally graded beams with non-uniform cross-section. Journal of Sound and Vibration 329, 2291–2303 (2010)
[20] Korak Sarkar, Ranjan Ganguli. Closed-form solutions for non-uniform Euler–Bernoulli free–free beams. Journal of Sound and Vibration 332, 6078–6092 (2013)
[21] S. Rajasekaran. Buckling and vibration of axially functionally graded nonuniform beams using differential transformation based dynamic stiffness approach. Meccanica 48, 1053–1070 (2013)
[22] Samir AL-Sadder, Raid A. Othman AL-Rawi. Finite difference scheme for large-deflection analysis of non-prismatic cantilever beams subjected to different types of continuous and discontinuous loadings. Archive of Applied Mechanics 75, 459–473 (2006)
[23] J. Awrejcewicz, A.V. Krysko, J. Mrozowski, O.A. Saltykova, M.V. Zhigalov. Analysis of regular and chaotic dynamics of the Euler–Bernoulli beams using finite difference and finite element methods. Acta Mechanica Sinica 27(1), 36–43 (2011)
[24] Meirovitch L. Fundamentals of vibrations. McGraw-Hill, New York (2001)
[25] Yong Huang, Ling-E Yang, Qi-Zhi Luo. Free vibration of axially functionally graded Timoshenko beams with non-uniform cross-section. Composites: Part B 45, 1493–1498 (2013)